Towards realization of an Energy Internet: Designing distributed energy systems using game-theoretic approach

Applied Energy xxx (xxxx) xxx

Contents lists available at ScienceDirect

Applied Energy

journal homepage: www.elsevier.com/locate/apenergy

Towards realization of an Energy Internet: Designing distributed energy systems using game-theoretic approach

A.T.D. Perera [a,*], Z. Wang [b], Vahid M. Nik [c,d,e], Jean-Louis Scartezzini [f]

[a] Urban Energy Systems Laboratory, EMPA, Überland Str. 129, 8600 Dübendorf, Switzerland
[b] Imperial College Business School, Imperial College London, UK
[c] Division of Building Technology, Department of Architecture and Civil Engineering, Chalmers University of Technology, SE-41296 Gothenburg, Sweden
[d] Division of Building Physics, Department of Building and Environmental Technology, Lund University, SE-22363 Lund, Sweden
[e] Institute for Future Environments, Queensland University of Technology, Garden Point Campus, 2 George Street, Brisbane, QLD 4000, Australia
[f] Solar Energy and Building Physics Laboratory (LESO-PB), Ecole Polytechnique Fédérale de Lausanne (EPFL), CH-1015 Lausanne, Switzerland

HIGHLIGHTS

- Novel distributed optimization algorithm for energy planning.
- Each energy system is considered as agent interacting with Energy Internet.
- Consider both cooperative (FCS) and non-cooperative (NCS) scenario.
- FCS and NCS reduce the cost respectively by 30% and 15% compared present methods.

ARTICLE INFO

Keywords:
Distributed power generation
Multi-agent systems
Game-theory
Power system planning,

ABSTRACT

Distributed energy systems play a significant role in the integration of renewable energy technologies. The Energy Internet links a fleet of distributed energy systems to each other and with the grid. Interactions between the distributed energy systems via information sharing could significantly enhance the efficiency of their real-time operation. However, privacy and security concerns hinder such interactions. A game-theoretic approach can help in this regard, and enable consideration of some of these factors when maintaining interactions between energy systems. Although a game-theoretic approach is used to understand energy systems' operation, such complex interactions between the energy systems are not considered at the early design phase, leading to many practical problems, and often leading to suboptimal designs. The present study introduces a game-theoretic approach that enables consideration of complex interactions among energy systems at the early design phase. Three different architectures are considered in the study, i.e., energy eystem prior to grid (ESPG), fully cooperative (FCS), and non-cooperative (NCS) scenarios, in which each distributed energy system is taken as an agent. A novel distributed optimization algorithm is developed for both FCS and NCS. The study reveals that FCS and NCS reduce the cost, respectively, by 30% and 15% compared to ESPG. In addition to cost reduction, there is a significant change in the energy system design when moving from FCS to NCS scenarios, clearly indicating the requirement for a scenario that lies between NCS and FCS. This will lead to reducing design costs while maintaining privacy.

1. Introduction

Integration of renewable energy technologies into the energy infrastructure has been extensively discussed recently due to the rapid depletion of fossil fuel resources and environmental concerns [1,2]. Previously, large-scale integration of non-dispatchable renewable energy technologies was often followed up reinforcing of the grid, which imposes economic constraints. Furthermore, maintaining a reliable and robust operation is a challenge following the large-scale integration of non-dispatchable energy technologies. Distributed energy systems, such as micro-grids and energy hubs, have become an attractive solution in this context because they have shown the potential to integrate higher

* Corresponding author.
E-mail address: dasun.perera@empa.ch (A.T.D. Perera).

https://doi.org/10.1016/j.apenergy.2020.116349
Received 17 August 2020; Received in revised form 23 November 2020; Accepted 9 December 2020

fractions of non-dispatchable energy technologies [3,4]. Both dispatchable energy technologies and energy storage devices help to withstand the fluctuations in demand and generation with a minimum impact on the grid [5]. However, designing distributed energy systems that consist of different energy technologies is a difficult task.

For the energy transition, it is essential to scale up the implementation of distributed energy systems, catering to local energy demand while harnessing renewable energy potential. To this effect, the energy system's design needs to consider the interactions between systems (through multi-energy grids). Designing such an energy infrastructure is a significant challenge for two main reasons:

- Expansion of the decision space that needs to be explored;
- Difficulties in considering the interactions among energy systems.

Moving from a single distributed energy system to a set of energy systems interacting with each other extends the decision space. Both connectivity and strength of the network need to be optimized in this context. This expansion of the decision space makes the optimization process more challenging. Maroufmashat et al. [6] conducted a simultaneous optimization of energy systems and their energy network in a case study consisting of three distributed energy systems. Similarly, several studies have focused on the simultaneous optimization of energy systems and networks. Many recent studies have also focused on using multi-agent systems with fully cooperative scenarios to understand the complex interactions between energy systems concerning the operation. All of these studies consider the fully cooperative mode in design and operation. A fully cooperative scenario considers that all of the decisions related to the entire energy infrastructure are made by one entity. The distributed energy systems (agents) act in a fully transparent manner without maintaining any privacy.

Energy markets are gradually shifting to a more open environment in which distributed energy systems behave as agents with much higher autonomy. Consequently, the fully cooperative scenario will misrepresent the transition in the energy sector [6,7]. A bargaining process of different agents is often considered during decision making through agent-based models. Furthermore, non-cooperative scenarios will accommodate sustainable energy technologies depending upon the agents' preferences while guaranteeing each energy system's reliable and robust operation. Moving to a non-cooperative strategy will help to study liberalized energy markets. Therefore, such a representation is essential for realizing the broader Energy Internet, in which different stakeholders related to energy services meet each other in a common energy market.

Several recent studies have focused on non-cooperative games in the real-time operation of distributed energy systems (dispatch problem), raising a number challenges to the optimization process compared to cooperative scenarios. Khan and Pasupuleti [8] used non-cooperative game theory to manage the operation within a distributed energy system. The focus of their work was to minimize the operation of the fossil fuel-based generator. Liu et al. [9] moved beyond the boundary of a single energy system and considered the interactions among several energy systems. Motelleb et al. [10] extended the concept by considering the network to be constrained. They used the networked Stackelberg game for this purpose. Hanmin et al. [11] considered a similar problem with thermal networks. In addition, the non-cooperative scenario has been considered for the optimal dispatch of polygeneration [12], energy storage management [13], microgrid energy management with the day-ahead energy market [14], voltage control of standalone microgrids [15], etc. A comprehensive explanation of these applications can be found in a recent review by He et al. [16]. However, these studies are limited to the operation of energy systems. Therefore, the influence of their design on control has not been discussed. Although it is not comprehensive, a game-theoretic approach has been used to design energy systems. Jing et al. [17] conducted energy system optimization considering the cooperative scenario and represented distributed energy systems using multiple agents during the decision-making process. Mohseni et al. used a fully cooperative scenario to optimize a distributed energy system, regarding each component as an agent [18]. Jin et al. [19] compared cooperative and non-cooperative scenarios to design a distributed energy system using the Particle Swarm method.

Moving from a single energy system or a microgrid to an Energy Internet (Fig. 1a) complicates the design problem. For example, it is required to consider both design and operation of each energy system and the energy flow within the network. Wang and Perera [20,21] introduced a methodology to optimize the Energy Internet considering $n-1$ security. The optimization algorithm demonstrated the potential to optimize the Energy Internet with more than ten distributed energy systems, considering the cooperative scenario. However, the interactions between the grid and distributed energy systems are weakly considered in this study, which can easily lead to sub-optimal solutions. Furthermore, maintaining the privacy and the autonomy at the system level is essential, and is known to be the key to the progress of an Energy Internet, as suggested by Inderwildi et al. [22], where a non-cooperative approach could be beneficial. The model proposed by Wang and Perera [20,21] does not consider non-cooperative scenarios. The non-cooperative approach considers each agent (such as a distributed energy system) as a unit that tries to maximize its profit while interacting with an open energy market, including several such agents that do not cooperate. Designing energy systems for a non-cooperative energy market converts the optimization problem into a set of distributed optimization problems (in which each agent represents a distributed energy system). To achieve market equilibrium, the optimization process is conducted for several rounds until the Nash equilibrium is guaranteed. This will extend the computational time. Therefore, accommodating privacy and autonomy at the level of the local energy system is a challenging task, and vital to the energy transition.

Considering the importance of non-cooperative agents in realizing an Energy Internet and the importance of moving to a distributed architecture to design an Energy Internet, this study focuses on introducing a novel optimization algorithm. The results are compared between non-cooperative, enhanced cooperative, and the present state-of-the-art models (Wang and Perera [20,21]). The importance of moving to a distributed architecture to design an Energy Internet, and the impact of considering autonomy and privacy in the non-cooperative scenario, is discussed based on the Pareto solutions obtained using the three different techniques. The research paper is organized in the following manner: Section 2 presents the overview of the approach used for the coordinated design of an Energy Internet consisting of several distributed energy systems. Sections 3 and 4 illustrate the computational model, the optimization algorithm, and the results of the study.

2. Coordinated design and operation of energy systems for an Energy Internet

The concept of the Energy Internet has been developed to allow stronger interactions among multi-energy systems connected through multi-energy networks (Fig. 1a). An Energy Internet allows a higher integration level of renewable energy technologies while enabling self-healing and plug and play devices. The design and operation of the energy infrastructure play an important role in the process of realizing an Energy Internet in which cyber–physical interactions are considered. A multi-energy network supports physical interactions, whereas information exchange among the distributed energy systems enables cyber interactions with the support of communication technology. This requires making energy systems more intelligent. In addition, interactions among distributed energy systems are essential to provide the flexibility to integrate renewable energy technologies and cater to the requirement of prosumers. The Energy Internet design process can be conducted in different ways considering the interactions among the energy hubs within the Energy Internet. In this study, three scenarios are considered.

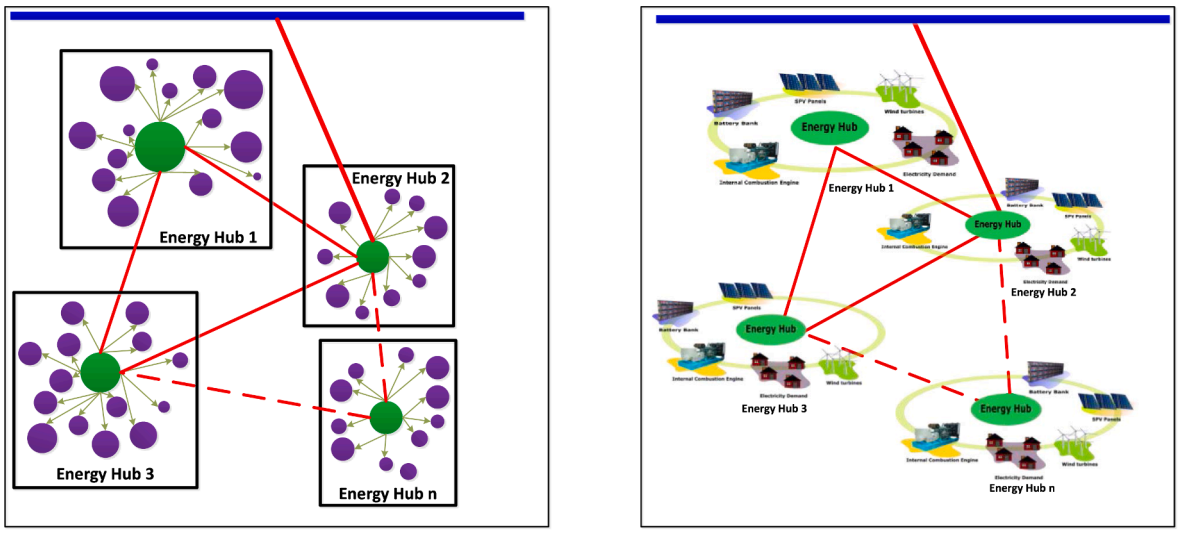

(a)

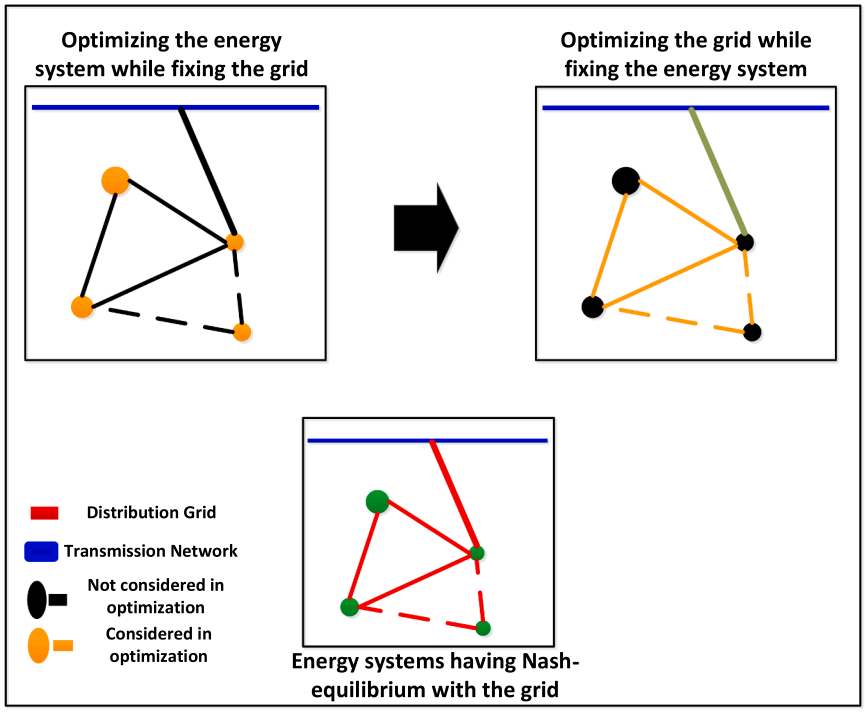

(b)

Fig. 1. In this figure, the outlay of the Energy Internet concept is presented in (a). Respectively, (b), (c), and (d) present the ESPG, non-cooperative, and fully cooperative scenarios used to design the Energy Internet.

2.1. Energy system optimization considering predefined grid curtailments (energy system prior to grid, ESPG)

The design of the Energy Internet requires simultaneous optimization of the energy systems and grid. Optimization needs to be performed at three levels to achieve this, i.e., 1) the operation of the energy systems, 2) the system configurations of the energy systems, and 3) the connectivity and strength of the network [23]. The Energy Internet design process is initiated as a process with two steps by Fazlollahi et al. [23], in which the energy system is optimized initially followed by the dispatch optimization using a bi-level optimization algorithm. Subsequently, the energy network (electricity or heat) is optimized as the second step. However, the influences of grid curtailments are not considered in detail at the first level, in which the energy system is optimized using the bi-level optimization algorithm. Perera et al. [24–26] extended this approach by considering predetermined grid

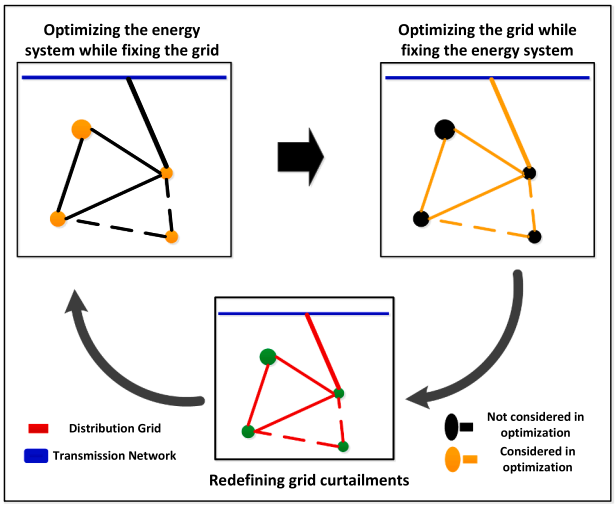

(c)

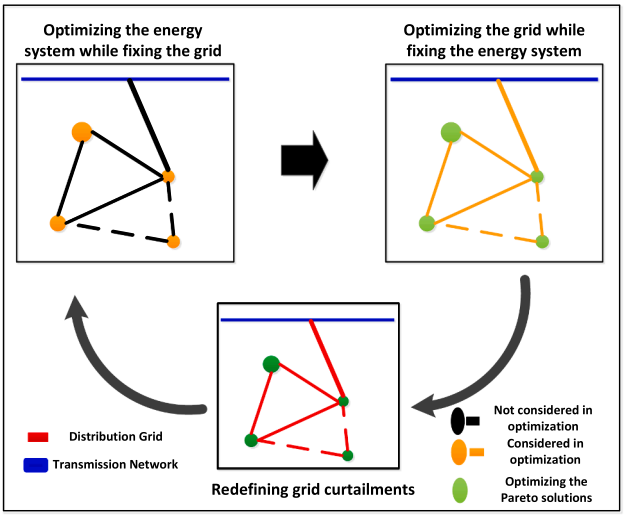

(d)

Fig. 1. (*continued*).

curtailments. Subsequently, Wang and Perera [20] optimized the energy system and network simultaneously considering n − 1 security of the Energy Internet. The ESPG scenario presents this approach in which the energy system is optimized initially considering a set of predetermined grid curtailments and, subsequently, the energy network is optimized, as shown in Fig. 1b. This approach has several drawbacks. The influences of network interactions and neighboring energy systems are disregarded in the optimization process. This may lead to significant congestion in the grid, resulting in a sub-optimal system design. Furthermore, a centralized intervention is used when optimizing the Energy Internet.

2.2. Fully cooperative scenario (FCS)

A fully cooperative scenario (FCS) facilitates the sharing of information among the agents through a centralized authority, so that each energy system is aware of the adjacent system. Usage of the grid, which allows purchasing and injection, is shared among all of the energy hubs with the support of the centralized authority. This enables each energy system to be optimized considering the influences of neighbors. Further, it provides more grid capacity whenever stronger interactions need to be maintained (as shown in Fig. 1c), in contrast to the ESPG. An iterative process is used to update the network and system design improves the objective functions compared to the ESPG.

2.3. Non-cooperative scenario (NCS)

The non-cooperative scenario falls between the FCS and ESPG. It does not have a centralized authority that provides comprehensive information about the neighboring energy systems and grid congestion during the energy system optimization. This allows privacy to be maintained. Energy systems interact with their neighboring energy systems to maximize their gains through participation in games. Limitations of the grid and influences of neighboring systems are understood while participating in the game (until one reaches the Nash equilibrium). An iterative process is introduced in this study for the NCS in which the grid and energy hub are optimized sequentially. Although the iterative process is similar to that of the FCS, the objective function and the decision space are limited to the grid connectivity and its cost

without considering the energy system (as performed in the FCS) in both objective and decision spaces (as shown in Fig. 1c). The NCS considers the network a separate agent similar to a distributed energy system, trying to minimize its cost while guaranteeing the flow constraints demanded by each distributed energy system (the competition exists among the energy systems and with the network agent to minimize their cost). This contrasts with the FCS in which a centralized agent selects the optimal energy system design for each location (from the Pareto solutions obtained for each energy system) and the network architecture. More details of these differences are explained in Section 3.

3. Modeling approach

The Energy Internet is assumed to consist of several energy hubs connected through the grid. However, each energy hub has its own distribution grid, which is not considered to simplify the study. This converts the design problem, as shown in Fig. 1 (a), in which each energy hub and its connectivity (between hubs) need to be optimized. However, the design optimization of the energy systems and grid, although allowing higher independence to the energy systems, is not a process that can be achieved in a single step. Hence, an iterative approach should be adopted when sequentially optimizing the energy systems' design and the connectivity in two different stages. A techno-economic model is developed to optimize the energy hub and the grid connecting the hubs. This section presents a brief overview of the techno-economic models for optimizing the energy system and network separately. Subsequently, the optimization algorithm is then explained.

3.1. The design problem of the distributed energy hub

Each energy hub studied consists of wind turbines, photovoltaic (PV) panels, a battery bank, and an internal combustion generator (ICG), and interacts with the transmission grid. Catering to both heating and electricity demands is considered in this study. It is assumed that heat pumps, which convert thermal demand into electricity demand, are used in all of the buildings. Upper and lower bounds for grid integration level (curtailments) and purchasing electricity are obtained on an hourly basis using the network model, depending upon the scenario (ESPG, FCS, or NCS).

3.1.1. Energy flow model

The energy system model consists of individual models for non-dispatchable components, dispatchable components, energy storage, and energy conversion devices such as heat pumps. Hourly global horizontal solar irradiation for each city is taken from the weather data stored in the meteorological database as explained in Section 3.4. This is used to compute the power generation from the photovoltaic (PV) panel, according to Eq. (1).

$$P_t^{PV,h} = G_t^{\beta,h}\,\eta_t^{PV,h}\,A^{PV,h}\,x^{PV,h}, \quad \forall t \in T\,\forall h \in H \tag{1}$$

In this equation, h ($\forall h \in H$) and t ($\forall t \in T$) denote the energy hub and time step. $G_t^{\beta,h}$ represents the total solar irradiation on a plane with tilt angle β. $A^{PV,h}$ and $x^{PV,h}$ ($x^{PV,h} \in X^h$) represent the area of a single PV panel and the number of PV panels in the energy system. $\eta_t^{PV,h}$ presents the efficiency of a PV panel, which depends on the type of the solar panel (materials used for manufacture), solar irradiation, cell temperature, air mass, and ambient temperature. A similar approach is used to compute the power generation from wind turbines. Power generation from the fleet of wind turbines ($P_t^{W,h}$) connected to the energy hub is computed using Eq. (2).

$$P_t^{W,h} = \widetilde{P_t^{W,h}}(v_t^h)\; x^{w,h}\,\eta^{W}, \forall t \in T\;\forall h \in H \tag{2}$$

where $x^{W,h}$ ($x^{W,h} \in X^h$) denotes the number of wind turbines, which is optimized using the optimization algorithm, and η^w accounts for other losses that take place in the energy conversion. $\widetilde{P_t^{W,h}}(v_t^h)$ denotes the power generation from a single wind turbine connected to the energy hub. v_t^h presents the wind speed at the wind turbine hub level. More details about the energy system model and the dispatch strategy are presented in Supporting Document A1 and A2.

3.1.2. Formulation of objective functions

Pareto optimization is conducted for the energy system considering two objective functions, i.e., cost and grid integration level. Net present value (NPV) is used as the financial indicator and grid interactions reflect the impact of the network interactions on the design of the energy system. Higher network interactions will increase the dependence of the energy system on the neighboring energy systems, whereas lower grid interactions will result in higher cost.

The net present value is used to present the financial performance of the system. The NPV is computed considering the initial capital cost (ICC) of the system, in addition to fixed, operation, and maintenance costs. The ICC of the complete system is calculated considering initial expenditure on system components ($\forall s \in S$: set of system components), such as wind turbines, PV panels, and battery bank. Regular maintenance costs of system components are considered under the fixed annual cash flow (MC^F). Replacement costs for ICG, battery bank (calculated based on the number of replacements), and power electronic devices are considered as a variable annual cash flow (MC^V). Finally, the present value of the operation and maintenance cash flows (for system components ($\forall s \in S$: set of system components) such as PV panels, wind turbines and ICG) is calculated according to Eq. (3), taking the lifetime of the project as 20 years.

$$NPV^h = \sum_{\forall s \in S} ICC_s^h + \sum_{\forall s \in S} MC_s^{F,h}\,CRF_s + \sum_{\forall k \in K}\sum_{\forall s \in S} p^k\,MC_s^V, \forall h \in H \tag{3}$$

In this equation, CRF denotes the capital recovery factor and p denotes the real interest rate. Finally, k represents the year considered. Finally, levelized energy cost (LEC) is derived by levelizing the NPV considering the entire energy demand serviced by the hub during its lifetime.

The energy hub interacts with the grid by selling and purchasing energy depending on fluctuations in energy demand and renewable potential. However, the limitations for the grid interactions are imposed depending on the strength of connectivity, demand, and generation of the other energy hubs. Grid curtailments for both injecting electricity to and purchasing it from the distribution network are considered as a constraint for the entire period in the ESPG scenario. However, these curtailments are updated during the iterative process for both NCS and FCS. The curtailments define the upper bound for the energy interactions. Within these upper bounds, the energy hub optimization algorithm looks for design solutions that can further minimize the grid interactions considering both export and import scenarios. Therefore, grid integration level (GI_{IG}^h) is defined according to Eq. (4), which is considered an objective function in the optimization.

$$GI_{IG}^h = \frac{\sum_{\forall t \in T} P_t^{IG,h} + P_t^{Ex,h}}{\sum_{\forall t \in T} P_t^{ELD,h}}, \forall h \in H \tag{4}$$

In this equation,$P_t^{IG,h}$, $P_t^{Ex,h}$, and $P_t^{ELD,h}$ denote energy imported and exported from the energy hub, and the electricity demand of the hub, respectively.

3.2. Distributed network planning problem

A common model is used to obtain the Pareto solutions for the energy hubs for each of NCS, FCS, and ESPG. The distributed network-planning problem is considered following the optimization of energy hubs, which it uses to update the grid curtailments, which is the exception of the ESPG scenario. For the ESPG scenario, fixed grid curtailments are considered during the energy hub optimization. Subsequently, the

network is optimized at the secondary level. A Pareto optimization is conducted considering two objective functions at the secondary level. Cost and autonomy levels are considered at this level. However, the formulation of the objective function is different when moving from one scenario to another, which is explained in detail in this section.

3.2.1. Formulating the cost of the Energy Internet

Each energy hub presents a set of Pareto solutions following the optimization, as explained in Section 3.1. The minimum cost of the entire Energy Internet depends on selecting the optimal Pareto solution for each hub and the network connecting the energy hubs. However, selecting the optimal system configuration for each energy hub requires a centralized intervention (sharing the details of the local energy hubs with the centralized body). Both ESPG and FCS scenarios consider the entire Energy Internet with this centralized intervention. This leads to the formulation of the NPV^{IE}, which is computed considering the net present value of all of the energy hubs and the operation and maintenance cost for the distributed network (Eq. (5)).

$$NPV^{IE}_{ESPG/FCS} = \sum_{\forall h \in H} NPV^{h} + \sum_{\forall l,m \in H} NPV^{x_{lm}} \tag{5}$$

In, Eq. (5), $NPV^{x_{lm}}$ denotes the installation, operation, and maintenances cost for the line connecting energy hubs l and m. NPV^{h} denotes the net present value of a single energy hub. The decision space for both the ESPG and the FCS consists of energy hub design d^{h} ($\forall d \in D^{h}, \forall h \in H$) for each energy hub and connectivity strength for $x_{lm}(\forall l, m \in H)$. x_{lm} presents the upper limit for the interactions maintained (maximum power exchanged) between the two hubs. Increasing this will help to improve the interactions between the hubs at an additional cost.

The NCS eliminates the possibility of a centralized intervention. Therefore, the network is considered as another agent (similar to an energy hub), which minimizes its cost and the interactions with the transmission network. As a result, the design configuration of each energy hub (d^{h} ($\forall d \in D^{h}, \forall h \in H$) is not considered in the decision space. The formulation only considers design, operation, and the maintenance of the network (NPV^{Net}_{NS}). Therefore, $x_{lm}(\forall l, m \in H)$ is considered in the decision space and the objective function is formulated as Eq. (6).

$$NPV^{Net}_{NS} = \sum_{\forall l,m \in H} NPV^{x_{lm}} \tag{6}$$

3.2.2. Formulation of grid interactions for the Energy Internet

Grid interactions maintained with the transmission network (IT) are computed in a similar manner for all three scenarios. Both selling and purchasing are minimized when reaching lower IT levels. Eq. (7) is used to compute the IT.

$$IT = \frac{\sum_{\forall t \in T} P^{IG,EI}_{t} + P^{EX,EI}_{t}}{\sum_{\forall h \in H} \sum_{\forall t \in T} P^{ELD}_{t,h}} \tag{7}$$

In this equation, $P^{IG,EI}_{t}$, $P^{EX,EI}_{t}$, and $P^{ELD}_{t,h}$, respectively, denote energy exported and imported from the transmission network, and the energy demand for each energy hub.

3.3. Optimization framework

The optimal design of an Energy Internet requires simultaneous optimization of distributed energy systems and the network connecting the distributed energy systems. Simultaneous optimization of both hubs and the network is a challenging task. Wang and Perera [20,21] proposed a three-level optimization algorithm to conduct optimization of such an Energy Internet, which is the starting point of the present study. Pareto optimization of the energy system is performed, which initially provides alternative design solutions for each energy hub, at the first step. The second step consists of two levels formulating a bi-level optimization algorithm. The primary level determines a combination of energy hubs taking one Pareto solution (derived in the first step) from each hub. Subsequently, a secondary algorithm calculates the optimal network connecting these energy hubs while guaranteeing an n − 1 security level. The total expenditure on the network can be obtained from the secondary level calculation, which feeds into the primary level to compute the total cost of the Energy Internet. Based on the total cost, the optimal system configuration of each energy hub is determined.

The main advantages of the computational model proposed by Wang and Perera [20,21] are its capability to scale up and its computational efficiency due to using a mixed integer linear program to solve the network optimization problem. The main limitation is that the first and second steps of the optimization algorithm are poorly linked with each other (Pareto solutions for the energy hubs at the first step are obtained without any understanding of the network capacities, which are determined at the second stage). As a result, the method can easily lead to sub-optimal solutions. Secondly, the fully cooperative scenario assumes that all of the information between different hubs and the centralized entities are shared, which is discouraged in certain instances. Due to these limitations, we moved beyond the model proposed by Wang and Perera [20,21]. Considering the ESPG, we chose a simplified version. The bi-level optimization proposed at the secondary level is replaced by a single optimization algorithm based on a heuristic method because the number of energy hubs considered in the study is small (which leads to a much smaller decision space, thus enabling the use of heuristic methods) compared to the previous work of Wang and Perera [20,21].

The novel optimization algorithm consists of three steps as shown in Fig. 2 in the supporting document (for FCS).

Step 1: The optimal energy system design for the energy hub is obtained considering the energy demand of the building stock, and wind and solar energy potential of the location on hourly scale. Pareto optimization leads to a set of alternative designs, which are arranged numerically with a descending net present value (NPV). Each alternative design might have a unique profile related to the manner in which it interacts with the grid. The manner in which it interacts with the grid depends on the grid integration level. The energy systems with a higher grid integration level will depend more on the grid, resulting in a higher cost for the grid. Two constraints are imposed when optimizing the distributed energy system, i.e.,

1) Loss of lead probability of the energy hub needs to be maintained within 0.1%;

2) Injecting to the grid and purchasing electricity from the grid should be maintained within certain limits. Each energy hub has such a set of alternative designs obtained through Pareto optimization of the energy hub. Step 1 is common for all of the scenarios. An evolutionary algorithm is used in this study to arrive at the Pareto front. Readers who are interested in further details about the formulation of the objective functions and methodology used for the optimization should see Ref. [24,25,27].

Step 2: This stage is devoted to optimizing the Energy Internet. The transportation model introduced by Romero et al. [28] is used in this study to model the grid. The basic formulation of the model used for the grid is presented in Wang and Perera et al. [20,21]. The Pareto sets determined by Step 1 are used as the input to Step 2. Each energy hub consists of a set of alternative solutions as explained in Step 1 (Step 2–1 in Fig. 2). The strength of the network, in addition to the system configuration for each hub, is optimized in Step 2 (Steps 2–2 and 2–3 in Fig. 2). Wang and Perera et al. [20,21] use a bi-level optimization algorithm for Step 2. The primary level of the optimization algorithm uses the Particle Swarm Algorithm (PSA) to optimize the system configuration, whereas the secondary level uses the mixed integer linear programing technique to optimize the network. In this study, a heuristic algorithm is used to optimize both system configuration and network. The difference of cooperative and non-cooperative scenarios arrives in this step. The cooperative scenario considers both system and grid in the optimization process (Fig. 2(c)) while the non-cooperative scenario considers only the grid (Fig. 2(b))

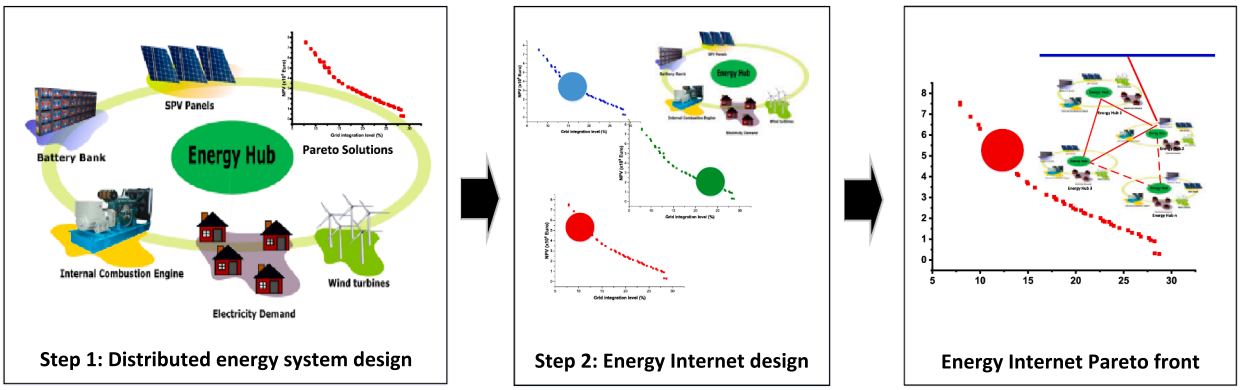

(a)

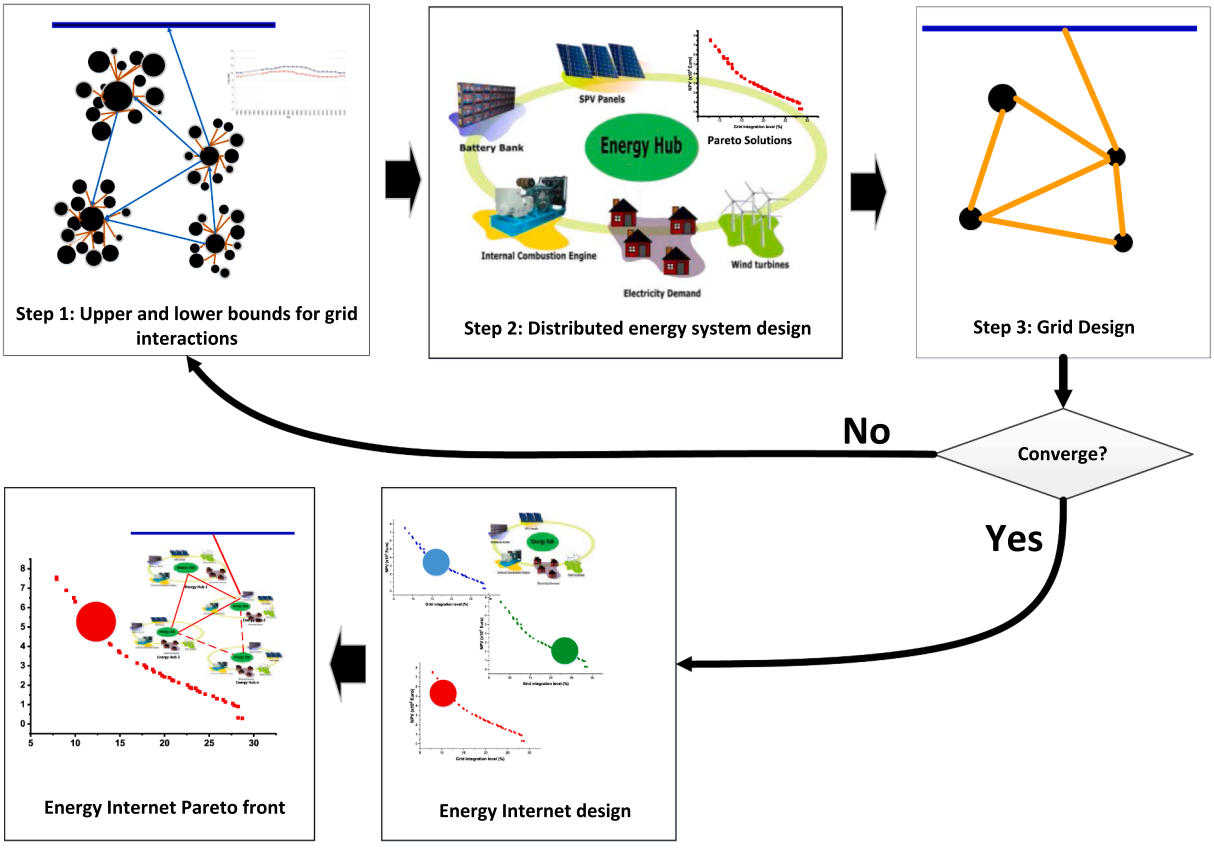

(b)

Fig. 2. Steps followed in the optimization algorithm. Respectively, Fig. 2 (a), (b) and (c) presents the steps followed in the (a) ESPG, (b) non-cooperative and (c) cooperative scenarios.

Step 3: The optimal Energy Internet obtained from Step 2 is used to arrive at the network capacities. The optimal network capacities obtained and the grid integration requirement for the energy hubs (obtained in Step 1) determine the power flow in each line during each time step, which is used to determine further allowances for grid injection and purchasing energy from the grid at each node. The allowances obtained at each time step are used to update the grid curtailments that are used in Step 1. Subsequently, the energy hubs are optimized again based on the updated grid curtailments.

The Step 1–3 is implemented iteratively in cycles for both cooperative and non-cooperative scenarios. A more straight forward approach is used in the ESPG (Fig. 2(a)) where there are no iterations. A comprehensive description about the optimization model used, decision space variables and the objective functions are presented in the Supporting Document (A2).

3.4. Outline of the case study

The three cities of Landskrona, Lund, and Malmö in southern Sweden are considered in this study to calculate the energy demand and renewable generation profiles. These cities have an oceanic climate with relatively mild winters compared to other locations at similar latitudes because of their proximity to the sea affected by the Gulf Stream. The type of weather data can affect the energy calculations considerably

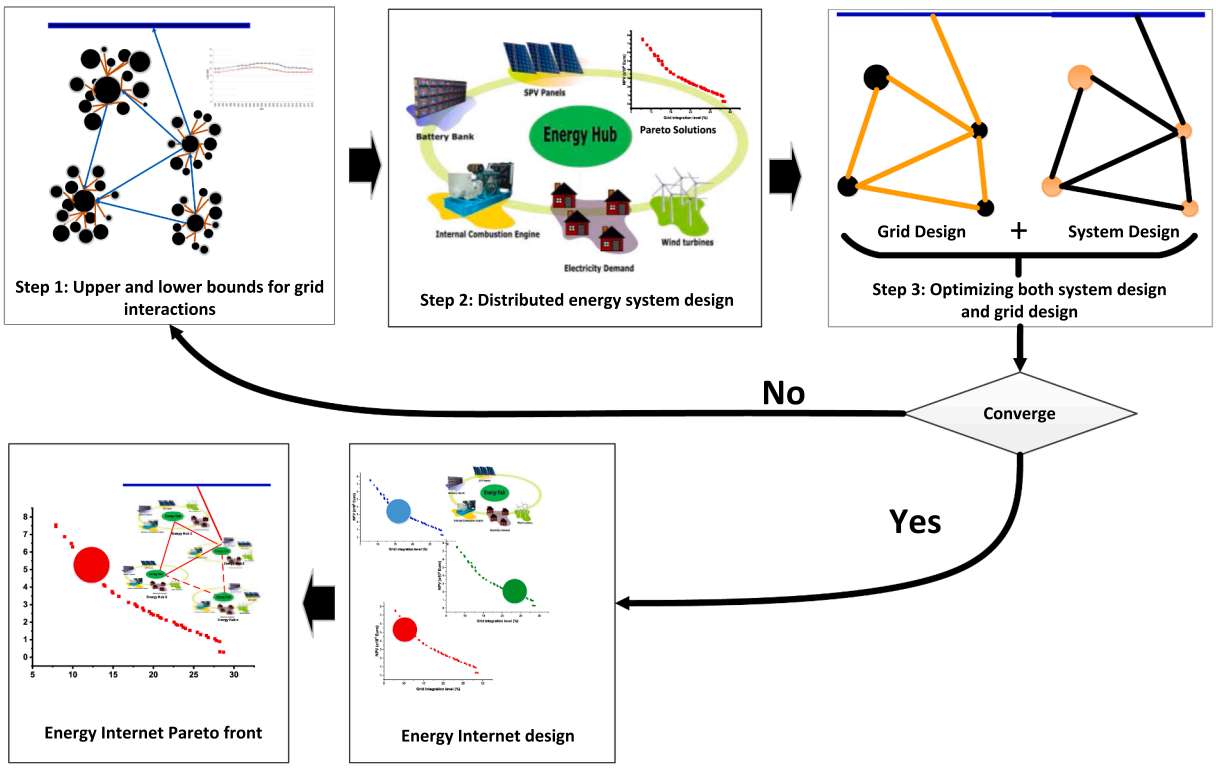

(c)

Fig. 2. (*continued*).

[29]. Future weather data sets were simulated by the RCA4 regional climate model with a spatial resolution of 12.5 km and downscaling four global climate models (GCMs)–namely, CNRM-CERFACS-CNRM-CM5, ICHEC-EC-EARTH, IPSL-IPSL-CM5A-MR, and MPI-M−MPI−ESM−LR−forced by two representative concentration pathways (RCPs) [30]; the first two are forced by RCP4.5 and RCP8.5, and the last two by RCP8.5. In total, six future climate scenarios were used to create one typical downscaled year (TDY) for each city during 2040–2069 (for more details, the reader is referred to [31]).

The energy demand of the residential buildings in a typical neighborhood in the cities was simulated considering a certain number of residential buildings in each city. The size of each neighborhood was set so that it did not exceed the peak energy demand of 420 kW. Accordingly, the neighborhoods in Landskrona, Lund, and Malmö, respectively, contain 39, 46, and 59 buildings that statistically represent the majority of residential buildings in each city. The models for building energy simulations were developed in the Simulink toolbox of MATLAB according to the BETSI investigation by the Swedish National Board of Housing, Building and Planning (Boverket, 2009) [32]. Simulations were conducted on an hourly time scale, with calculations of the total energy demand profiles, including the demand for heating, cooling, hot water, and fans, and considering if heat recovery is used in the building or not. The building simulations have been verified and used in some previous works (e.g., [33]).

4. Results and discussion

The energy systems' demand higher autonomy while expecting support from the grid whenever there is a shortage or excess in generation. Maintaining the optimum balance between these two objectives is difficult. It is interesting to analyze how the different scenarios introduced in this study help to balance autonomy while guaranteeing better connectivity to assist energy systems to withstand fluctuations in demand and generation.

4.1. Analyzing the fully cooperative scenario

The FCS considers the generation and demand of the other energy systems and the grid congestion during the optimization process as a centralized entity. As a result, it provides the opportunity to minimize the design and operation of the specific energy system, in addition to the entire system consisting of several energy hubs along with the grid. The LEC-GI (Grid Integration) Pareto front obtained for the four energy hubs is presented in Fig. 3. The obtained Pareto front shows a steep reduction

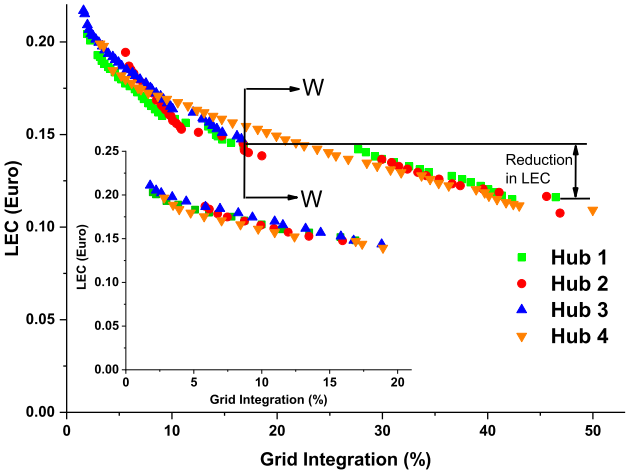

Fig. 3. Levelized Energy Cost and Grid Integration (LEC-GI) Pareto fronts obtained for the four hubs for the fully cooperative scenario (FCS) are given in the enlarged graph whereas the small graph presents the Pareto fronts for the Energy System Prior to Grid (ESPG) scenario. Pareto solutions to the left side of the W–W line are those introduced in the FCS, and result in a reduction in the LEC of around EUR 0.05.

in the LEC with the increase in grid interactions for design solutions that have grid interaction levels of less than 10%. The reduction in LEC is notably high for these design solutions compared to ESPG (a comprehensive analysis of the ESPG scenario is presented in Section A3, Supporting Document). For example, the LEC decreases from EUR 0.2042 to 0.1455 when the grid integration level is increased from 2 to 15.6% by reducing the LEC by 28% for Hub 1. In addition, the Pareto front obtained for the FCS yields design solutions with higher grid integration levels than those of ESPG. The Pareto solutions towards the right-hand side of the W–W line are the newly added designs when moving from the ESPG to FCS. For example, the grid integration level has increased from 16.9 to 46% with an increase of almost a factor of three when moving from the design solution with the highest grid interaction levels in Hub 1 under the ESPG scenario to the same design solution in the FCS. The higher grid interactions result in a significant drop in the LEC. For example, the LEC decreases from EUR 0.148 to 0.1161 when moving from the design solution with the highest grid interaction levels in Hub 1 under the ESPG scenario to the same design solution in the FCS, which is a drop of about 31%. Furthermore, a reduction in the LEC can be observed compared to Hub 4. These results clearly show that it is possible to notably reduce the lifecycle cost by improving the interactions with the neighboring energy hubs. The energy network plays a vital role in this context because it will enable higher interactions among different energy hubs.

The main advantage of the FCS is that the solutions obtained for each energy hub can be used to optimize the entire Energy Internet. The FCS presents Pareto solutions for each hub and the energy superstructure including all of the energy hubs and the grid. Hence, it is interesting to move from the Pareto solutions obtained for each energy hub to the optimum solutions obtained for the energy superstructure, which will provide a more holistic view. Thus, the two Pareto solutions showing the lowest LEC and grid interaction levels, respectively, for the entire energy superstructure are taken, and both the grid and energy system configurations of these solutions are tabulated in Table 1. Table 1 clearly demonstrates that there is a significant reduction in cost and a change in system configuration when moving from the ESPG to FCS.

4.2. Analyzing the non-cooperative scenario (NCS)

The design solutions obtained for the non-cooperative scenario fall between those of the ESPG and FCS. There are interactions among the energy systems and the grid, although these are not as strong as those in the FCS. Hence, it is important to analyze the changes in both energy hubs and the superstructure. To analyze the design solutions of the energy hubs, Pareto solutions for Hub 1 are plotted for both the FCS and NCS (Fig. 3). When analyzing the Pareto solutions, it is clear that the LEC obtained for the NCS is slightly higher than that of the solutions obtained for the FCS in many instances (marked in Region L). Furthermore, a few design solutions exist in which the FCS shows a slightly higher LEC, as marked in Region M. Finally, both Pareto fronts overlap each other when the grid interactions are very low and very high. To understand the possible causes for the deviation, three Pareto solutions with similar LEC are taken from each Pareto front (the FCS and NCS which belong to Region L) and tabulated in Table 2. When analyzing the design solutions, a significant increase in grid interactions can be observed when moving from the FCS to NCS for the same LEC. For example, GI increases from 5.2 to 9.31 when moving from F1 to N1, increasing the total grid interaction level by 80%. However, when comparing the grid purchasing levels, Pareto solutions that belong to the same case (with a similar LEC from the two different Pareto fronts) have similar grid purchasing levels. Therefore, the deviation is entirely due to the grid injection. This can be understood when comparing the grid injection levels of the Pareto solutions.

Further analysis of the scenarios showed that the increase in grid injection is due to the changes in the energy system design. The design solutions obtained for the NCS have a larger number of wind turbines compared to the FCS. For example, FC3 has 7 wind turbines whereas N3 has 28. The number of wind turbines has increased by a multiple by four and notably increased the grid injection. However, the LEC and grid purchase remain almost the same when moving from NS3 to FC3. NCS solutions accommodate more renewable energy technologies while maintaining more interactions with the grid, although the design solutions are dominated by the FCS. This clearly reflects the importance of coordination among the energy systems when incorporating renewable energy technologies and interacting with the neighboring energy systems. Continued the analysis considering the other three hubs is presented in Section A4 in the supporting document.

4.3. Analyzing the Energy Internet for NCS and FCS

A Pareto analysis of each hub presents an overview from a specific energy system perspective. However, it is important to consider the entire Energy Internet to obtain a more holistic understanding of the influences of cooperative and non-cooperative scenarios. This holistic assessment provides the opportunity to understand the impact of energy interactions among different energy hubs on the performance of the Energy Internet. Thus, NPV and interactions with the transmission network are plotted for the Pareto solutions of the Energy Internet in Fig. 4, which is followed by a detailed analysis taking several design solutions from the Pareto front in Table 3.

The Pareto front of NPV-IT presents the design solutions obtained considering the NPV of the Energy Internet (including the lifecycle cost of all of the different energy hubs and the grid) and the interactions the Energy Internet maintains with the transmission line for the FCS and NCS. When moving into the NCS, Pareto optimization is conducted considering the NPV of the grid and the interactions the Energy Internet maintains with the transmission line for the FCS. Hence, for the NCS, Fig. 5 presents the NPV of the Energy Internet for the Pareto solutions obtained considering the NPV of the grid and the IT. However, when analyzing Fig. 5, it is clear that the design solutions obtained for the NCS are non-dominant and present a Pareto front in the objective space of NPV-Energy Internet and the IT. Therefore, it is hereafter referred to as a Pareto front.

The Pareto fronts (FCS and NCS) overlap at the beginning where grid interactions are at a minimum. Subsequently, they divert from each other with the increase in grid interactions, resulting in a significant

Table 1
Pareto solutions having the lowest net present value (NPV) from the ESPG and FCS.

Scn	Hub	Pareto Sol^{n}	GI (%)	LEC (Euro)	Grid Inject (%)	Grid Purchase (%)	SPV*	WTC*	ICGC*
Low cost-FCS	1	FLCH1	29.9	0.14	13.4	16.6	84	4	60
	2	FLCH2	18.5	0.14	7.1	11.4	119	30	80
	3	FLCH3	3.9	0.19	2.4	1.6	37	0	100
	4	FLCH4	41.7	0.11	17.1	24.7	120	29	40
Opt. ESPG	1	ESH1	5.1	0.18	3.6	1.5	50	28	100
	2	ESH2	5.8	0.19	0.5	5.3	31	30	100
	3	ESH3	5.8	0.19	4.5	1.4	47	10	100
	4	ESH4	5.7	0.18	3.4	2.3	51	30	100

*In this table, SPV, WTC and ICGC respectively denote number of solar panels, number of wind turbines and the capacity of internal combustion generator.

Table 2
Three Pareto solutions having a similar LEC are taken from each Pareto front (FCS and NCS which belong to Region L).

Scn	Case	Pareto Sol^n	GI (%)	LEC (Euro)	Grid Inject (%)	Grid Purchase (%)	SPV*	WTC*	ICGC*
FCS	1	F1	5.20	0.180	3.628	1.571	54	13	100
NS	1	N1	9.31	0.180	8.069	1.246	57	29	100
FCS	2	F2	8.71	0.162	7.223	1.492	110	6	100
NS	2	N2	13.68	0.162	12.100	1.583	120	30	100
FCS	3	F3	16.81	0.144	7.340	9.473	120	7	80
NS	3	N3	20.91	0.146	11.863	9.048	120	28	80

*In this table, SPV, WTC and ICGC respectively denote number of solar panels, number of wind turbines and the capacity of internal combustion generator.

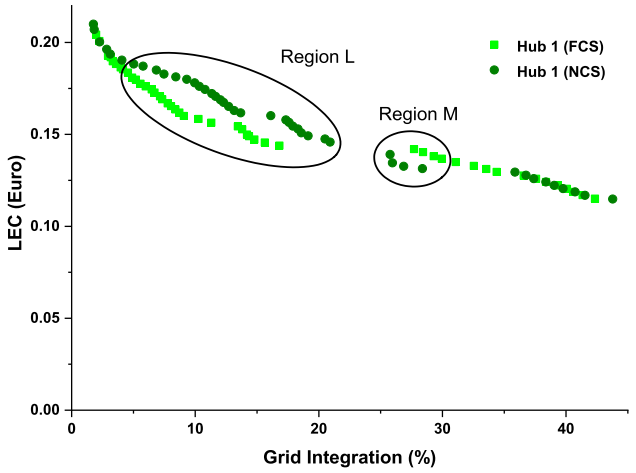

Fig. 4. A comparison of Pareto solutions for Hub 1 for FCS and NCS scenarios.

Table 3
Connectivity strength of each energy hub for the selected designs, NPV, and grid interactions maintained with the transmission line for the Energy Internet.

Scenario	Name	NPV (x10^6)	IT (MWh /year)	Hub 1 (kW)	Hub 2 (kW)	Hub 3 (kW)	Hub 4 (kW)
FCS	FIT 1	17.35	249	290	100	270	60
	FIT 2	15.74	589	290	190	280	90
	FIT 3	15.26	966	290	160	280	190
NCS	NIT1	18.58	257	280	20	210	60
	NIT2	17.73	582	280	20	210	60
	NIT3	16.16	968	240	80	280	60

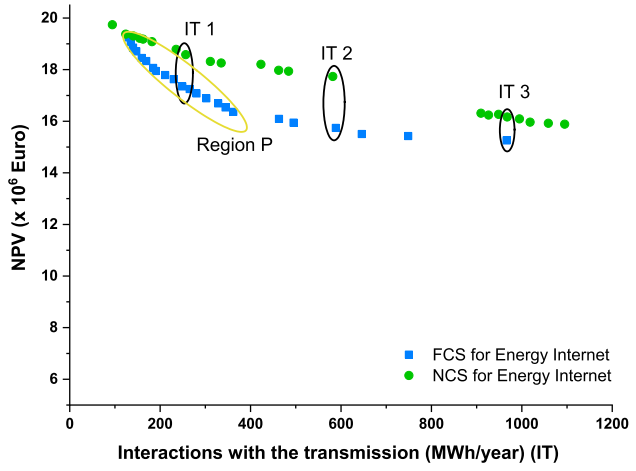

Fig. 5. A comparison of the two Pareto fronts obtained for the Energy Internet considering the FCS and NCS scenarios.

difference in NPV of up to 13%. A notable reduction in NPV is observed for the FCS with the increase in the IT in Region P. However, the difference between NPVs gradually decreases when reaching the end of the Pareto front where grid interactions are at a maximum.

It is of interest to further assess the impacts of the two different operation scenarios on the design of two energy hubs. Thus, the optimal design of each energy hub within IT 1, IT 2, and IT 3 are taken for both the FCS and NCS (as presented in Tables 4 and 5). A notable difference in grid interactions, cost, and system configurations can be observed for the energy hubs when comparing the NCS and FCS scenarios. It is observed that four hubs will have a unique system design under the FCS, whereas Hubs 3 and 4 will have the same design as that for NIT 1, 2, and 3 design solutions. The design solutions obtained for Hubs 3 and 4 (NIT 1–3–3 and NIT 1–3–4) are the Pareto solutions with the lowest grid integration level and the highest LEC. Moving from the NCS to FCS, Pareto solutions obtained for the energy hubs are neither the cheapest nor the most autonomous. A significant change in the LEC is observed when moving from one solution to another within the energy hub, including Energy Hubs 3 and 4. For example, the LEC decreases from EUR 0.185 to 0.113 when moving from FIT 1–4 to FIT 3–4. More importantly, the lowest LEC is observed for Hub 2 (Solution FIT1-2 for Grid Scenario FIT 1) and Hub 4 (Solution FIT2-4 and FIT3-4 for Grid Scenarios FIT 2 and 3) in the FCS. Hence, it is clear that utilizing the local renewable energy potential reduces the LEC, which is the opposite behavior from that of the NCS. Furthermore, the grid interactions of Hubs 2, 3, and 4 improve significantly compared to the NCS. GI reaches 41.74% (FIT 3–4) and 12.93% (FIT 2–3), respectively, for Hubs 3 and 4 for the FCS, and was below 3% for NIT1-3–3 and NIT1-3–4. As a result, a significant improvement in renewable energy capacity can be observed for Hubs 3 and 4. The design solutions obtained for FCS complement each other to operate the Energy Internet as a single energy hub. This can be observed in the three Pareto solutions for Hubs 3 and 4. FIT 1–3 and FIT 3–3 do not have any wind turbines whereas FIT 1–4 and FIT 3–4 have 29 wind turbines each. In contrast, FIT 2–3 has 30 wind turbines and FIT 2–4 does not have any. From a system design perspective, this clearly indicates proper organization between the energy hubs for the

Table 4
System configuration for three Pareto solutions obtained for the FCS.

	Name	LEC (Euro)	GI (%)	GP (%)*	SPV*	WTC*	ICGC*
Hub 1	FIT 1–1	0.181	4.90	1.53	52	13	100
	FIT 2–1	0.162	8.71	1.49	110	6	100
	FIT 3–1	0.137	29.95	16.56	84	4	60
Hub 2	FIT 1–2	0.153	10.91	4.40	120	30	100
	FIT 2–2	0.151	12.52	5.21	120	30	100
	FIT 3–2	0.138	18.54	11.41	119	30	80
Hub 3	FIT 1–3	0.190	4.61	1.49	41	0	100
	FIT 2–3	0.159	12.93	5.34	86	30	80
	FIT 3–3	0.194	3.95	1.60	37	0	100
Hub 4	FIT 1–4	0.185	4.39	2.93	38	29	100
	FIT 2–4	0.142	23.80	7.38	111	0	100
	FIT 3–4	0.113	41.74	24.69	120	29	40

*In this table, GP, SPV, WTC and ICGC respectively denote grid purchased electricity as a percentage of the annual energy demand, number of solar panels, number of wind turbines and the capacity of internal combustion generator.

Table 5
System configuration for three Pareto solutions obtained for the FCS. The system configuration of Hub 3 and 4 does not change when moving from IT 1 to IT 2 and IT 3.

	Name	LEC (Euro)	GI (%)	GP* (%)	SPV*	WTC*	ICGC*
Hub 1	NIT 1–1	0.147	20.51	8.58	120	26	80
	NIT 2–1	0.119	40.73	22.89	118	29	40
	NIT 3–1	0.105	53.35	32.60	120	30	20
Hub 2	NIT 1–2-2	0.211	2.93	2.64	28	30	120
	NIT 3–2-2	0.113	50.56	33.52	114	30	40
Hub 3	NIT 1–3-3	0.217	1.56	1.49	22	23	100
Hub 4	NIT 1–3-4	0.206	2.82	2.81	24	30	100

*In this table, GP, SPV, WTC and ICGC respectively denote grid purchased electricity as a percentage of the annual energy demand, number of solar panels, number of wind turbines and the capacity of internal combustion generator.

FCS, which enables them to coordinate their operation properly, as an Energy Internet.

4.4. Limitations of the study

The present study does not consider the influence of uncertainties imposed by the climate, instrumentation outage, energy market, etc. According to Perera et al. [34], uncertainties due to external factors can notably influence the energy system's performance, especially during extreme events [35]. Maintaining a robust operation of the Energy Internet is a significant challenge in this regard [20]. The present study also does not consider performance changes due to the uncertainties arising during the optimization process. Furthermore, the impact of extreme events on the infrastructure (vulnerability to cascade failures) and resilience is not considered in the present study. Considering these limitations will be an important extension of the present study that will immensely help the realization of the Energy Internet.

5. Conclusions and future perspectives

The Energy Internet is an emerging area of research that allows large-scale penetration of non-dispatchable renewable energy technologies such as wind and PV. Although several studies have focused on the operation of an Energy Internet consisting of several distributed energy systems, a comprehensive study has not been conducted on promising techniques that can be used to design such an Energy Internet. To help address this research gap, this study introduces a distributed optimization algorithm that can be used to optimize an Energy Internet. Then, three design strategies are considered assuming different behaviors for the distributed energy systems (agents), namely: (1) an energy system design with a predefined grid curtailments (ESPG) scenario, (2) a fully cooperative scenario (FCS), and (3) a non-cooperative scenario (NCS). The results obtained from this study reveal that Energy Internet design using the ESPG scenario causes levelized energy costs to be up to 30% higher compared to the FCS because of the lack of proper coordination between the grid and distributed energy hubs. Hence, it is essential to develop more effective methods that can reduce the cost by improving the interaction among the energy hubs. The FCS presents results which are opposite to those of the ESPG scenario, i.e., in the FCS, energy hubs interact efficiently with the grid and neighboring energy hubs.

The assessment conducted in the study reveals that the concept of the Energy Internet enables the co-existence of distributed energy systems while enabling higher renewable energy integration levels. A significant improvement in renewable energy integration and a reduction in levelized energy costs can be achieved through the NCS and FCS in which distributed optimization algorithms help achieve optimum designs. The FCS provides a better opportunity for all of the energy hubs irrespective of their distance from the transmission line. Furthermore, the FCS enables stronger interactions between energy hubs. However, it should be understood that stronger interactions may often lead to stronger dependencies. As a result, there is a tendency for cascade failures whenever one or several energy hubs fail to operate according to the expectations of the Energy Internet. Hence, methods to improve resilience while maintaining the interactions should be investigated. Hierarchical operation of distributed energy systems combined with a leader–follower strategy might be promising in this regard.

CRediT authorship contribution statement

A.T.D. Perera: Conceptualization, Methodology, Formal analysis, Writing - original draft. **Z. Wang:** Data curation, Writing - review & editing. **Vahid M. Nik:** Data curation, Writing - original draft. **Jean-Louis Scartezzini:** Supervision, Project administration, Writing - review & editing.

Declaration of Competing Interest

The authors declare that they have no known competing financial interests or personal relationships that could have appeared to influence the work reported in this paper.

Appendix A. Supplementary material

Supplementary data to this article can be found online at https://doi.org/10.1016/j.apenergy.2020.116349.

References

[1] Ćosić B, Krajačić G, Duić N. A 100% renewable energy system in the year 2050: The case of Macedonia. Energy 2012;48:80–7. https://doi.org/10.1016/j.energy.2012.06.078.
[2] Lund H, Mathiesen BV. Energy system analysis of 100% renewable energy systems—The case of Denmark in years 2030 and 2050. Energy 2009;34:524–31. https://doi.org/10.1016/j.energy.2008.04.003.
[3] Sansavini G, Piccinelli R, Golea LR, Zio E. A stochastic framework for uncertainty analysis in electric power transmission systems with wind generation. Renewable Energy 2014;64:71–81. https://doi.org/10.1016/j.renene.2013.11.002.
[4] Zio E, Sansavini G. Vulnerability of smart grids with variable generation and consumption: a system of systems perspective. IEEE Trans Syst, Man, Cybernetics: Syst 2013;43:477–87. https://doi.org/10.1109/TSMCA.2012.2207106.
[5] Guen ML, Mosca L, Perera ATD, Coccolo S, Mohajeri N, Scartezzini J-L. Improving the energy sustainability of a Swiss village through building renovation and renewable energy integration. Energy Build 2018;158:906–23. https://doi.org/10.1016/j.enbuild.2017.10.057.
[6] Zhou K, Yang S, Shao Z. Energy Internet: The business perspective. Appl Energy 2016;178:212–22. https://doi.org/10.1016/j.apenergy.2016.06.052.
[7] Huang AQ, Crow ML, Heydt GT, Zheng JP, Dale SJ. The future renewable electric energy delivery and management (FREEDM) system: the energy internet. Proc IEEE 2011;99:133–48. https://doi.org/10.1109/JPROC.2010.2081330.
[8] Basir Khan MR, Jidin R, Pasupuleti J, Shaaya SA. Optimal combination of solar, wind, micro-hydro and diesel systems based on actual seasonal load profiles for a resort island in the South China Sea. Energy 2015;82:80–97. https://doi.org/10.1016/j.energy.2014.12.072.
[9] Liu W, Gu W, Wang J, Yu W, Xi X. Game theoretic non-cooperative distributed coordination control for multi-microgrids. IEEE Trans Smart Grid 2018;9:6986–97. https://doi.org/10.1109/TSG.2018.2846732.
[10] Motalleb M, Siano P, Ghorbani R. Networked stackelberg competition in a demand response market. Appl Energy 2019;239:680–91. https://doi.org/10.1016/j.apenergy.2019.01.174.
[11] Cai H, You S, Wu J. Agent-based distributed demand response in district heating systems. Appl Energy 2020;262:114403. https://doi.org/10.1016/j.apenergy.2019.114403.
[12] Karavas C-S, Arvanitis K, Papadakis G. A game theory approach to multi-agent decentralized energy management of autonomous polygeneration microgrids. Energies 2017;10:1756. https://doi.org/10.3390/en10111756.
[13] Zheng Y, Hill DJ, Dong ZY. Multi-agent optimal allocation of energy storage systems in distribution systems. IEEE Trans Sustainable Energy 2017;8:1715–25. https://doi.org/10.1109/TSTE.2017.2705838.
[14] Dou C-X, Jia X-B, Li H, Lv M-F. Multi-agent system based energy management of microgrid on day-ahead market transaction. Electr Power Compon Syst 2016;44:1330–44. https://doi.org/10.1080/15325008.2016.1158216.

[15] Bhargavi KM, Jayalakshmi NS. Leader–follower-based distributed secondary voltage control for a stand-alone PV and wind-integrated DC microgrid system with EVs. J Control Autom Electr Syst 2020;31:233–46. https://doi.org/10.1007/s40313-019-00530-6.
[16] He J, Li Y, Li H, Tong H, Yuan Z, Yang X, et al. Application of game theory in integrated energy system systems: a review. IEEE Access 2020;8:93380–97. https://doi.org/10.1109/ACCESS.2020.2994133.
[17] Jing R, Wang M, Liang H, Wang X, Li N, Shah N, et al. Multi-objective optimization of a neighborhood-level urban energy network: Considering Game-theory inspired multi-benefit allocation constraints. Appl Energy 2018;231:534–48. https://doi.org/10.1016/j.apenergy.2018.09.151.
[18] Mohseni S, Moghaddas-Tafreshi SM. A multi-agent system for optimal sizing of a cooperative self-sustainable multi-carrier microgrid. Sustain Cities Soc 2018;38:452–65. https://doi.org/10.1016/j.scs.2018.01.016.
[19] Jin S, Wang S, Fang F. Game theoretical analysis on capacity configuration for microgrid based on multi-agent system. Int J Electr Power Energy Syst 2021;125:106485. https://doi.org/10.1016/j.ijepes.2020.106485.
[20] Wang Z, Perera ATD. Integrated platform to design robust energy internet. Appl Energy 2020;269:114942. https://doi.org/10.1016/j.apenergy.2020.114942.
[21] Wang Z, Perera ATD. Robust optimization of power grid with distributed generation and improved reliability. Energy Procedia 2019;159:400–5. https://doi.org/10.1016/j.egypro.2018.12.069.
[22] Inderwildi O, Zhang C, Wang X, Kraft M. The impact of intelligent cyber-physical systems on the decarbonization of energy. Energy Environ Sci 2020;13:744–71. https://doi.org/10.1039/C9EE01919G.
[23] Fazlollahi S, Becker G, Maréchal F. Multi-objectives, multi-period optimization of district energy systems: III. Distribution networks. Comput Chem Eng 2014;66:82–97. https://doi.org/10.1016/j.compchemeng.2014.02.018.
[24] Perera ATD, Nik VM, Mauree D, Scartezzini J-L. Electrical hubs: An effective way to integrate non-dispatchable renewable energy sources with minimum impact to the grid. Appl Energy 2017;190:232–48. https://doi.org/10.1016/j.apenergy.2016.12.127.
[25] Perera ATD, Nik VM, Mauree D, Scartezzini J-L. An integrated approach to design site specific distributed electrical hubs combining optimization, multi-criterion assessment and decision making. Energy 2017;134:103–20. https://doi.org/10.1016/j.energy.2017.06.002.
[26] Perera ATD, Coccolo S, Scartezzini J-L, Mauree D. Quantifying the impact of urban climate by extending the boundaries of urban energy system modeling. Appl Energy 2018;222:847–60. https://doi.org/10.1016/j.apenergy.2018.04.004.
[27] Perera ATD. Modeling and assessment of urban energy systems. Infoscience 2019. https://doi.org/10.5075/epfl-thesis-9389.
[28] Romero R, Monticelli A, Garcia A, Haffner S. Test systems and mathematical models for transmission network expansion planning. Transmission and Distribution IEE Proceedings - Generation 2002;149:27–36. https://doi.org/10.1049/ip-gtd:20020026.
[29] Moazami A, Nik VM, Carlucci S, Geving S. Impacts of future weather data typology on building energy performance – Investigating long-term patterns of climate change and extreme weather conditions. Appl Energy 2019;238:696–720. https://doi.org/10.1016/j.apenergy.2019.01.085.
[30] Giorgetta MA, Jungclaus J, Reick CH, Legutke S, Bader J, Böttinger M, et al. Climate and carbon cycle changes from 1850 to 2100 in MPI-ESM simulations for the Coupled Model Intercomparison Project phase 5. J Adv Model Earth Syst 2013;5:572–97. https://doi.org/10.1002/jame.20038.
[31] Nik VM. Application of typical and extreme weather data sets in the hygrothermal simulation of building components for future climate – A case study for a wooden frame wall. Energy Build 2017;154:30–45. https://doi.org/10.1016/j.enbuild.2017.08.042.
[32] BETSI. Description of the existing buildings: technical characteristics, indoor environment and energy consumption. (Bebyggelsens energianvändning, tekniska status och innemiljö). Karlskrona, Sweden: Boverket – the National Board of Housing, Building and Planning; 2009.
[33] Nik VM, Mata É, Sasic Kalagasidis A. A statistical method for assessing retrofitting measures of buildings and ranking their robustness against climate change. Energy Build 2015;88:262–75. https://doi.org/10.1016/j.enbuild.2014.11.015.
[34] Perera ATD, Nik VM, Wickramasinghe PU, Scartezzini J-L. Redefining energy system flexibility for distributed energy system design. Appl Energy 2019;253:113572. https://doi.org/10.1016/j.apenergy.2019.113572.
[35] Perera ATD, Nik VM, Chen D, Scartezzini J-L, Hong T. Quantifying the impacts of climate change and extreme climate events on energy systems. Nat Energy 2020;5:150–9. https://doi.org/10.1038/s41560-020-0558-0.